Results from the Pan-STARRS Orthogonal Transfer Array (OTA)

John L. Tonry[a], Barry E. Burke[b], Sidik Isani[a], Peter M. Onaka[a], Michael J. Cooper[b]

[a]Institute for Astronomy, University of Hawaii, 2680 Woodlawn Drive, Honolulu, HI 96822;
[b]Lincoln Laboratory, Massachusetts Institute of Technology

ABSTRACT

The Pan-STARRS project has completed its first 1.4 gigapixel mosaic focalplane CCD camera using 60 Orthogonal Transfer Arrays (OTAs). The devices are the second of a series of planned development lots. Several novel properties were implemented into their design including 4 phase pixels for on-detector tip-tilt image compensation, selectable region logic for standby or active operation, relatively high output amplifier count, close four side buttable packaging and deep depletion construction. The testing and operational challenges of deploying these OTAs required enhancements and new approaches to hardware and software. We compare performance achieved with that which was predicted, and discuss on-sky results, tools developed, shortcomings, and plans for future OTA features and improvements.

Keywords: Pan-STARRS, OTA, Orthogonal-Transfer CCD, tip tilt, gigapixels

1. THE OTA

The Orthogonal Transfer[1] Array (OTA) is a device which consists of an 8×8 array of 600×600 pixel CCDs. Each CCD (known as a "cell") is equipped with logic which isolates it or connects it to the output circuitry. The OTA subtends therefore about 5K $\times$ 5K pixels worth of sky, with inter-cell and inter-device gaps which reduce the fill factor to about 90%. This is a small loss of etendue compared to, for example, a 70% duty cycle of integration versus read time. A fast read time results from the output density. PSF improvements resulting from unique on-chip image correction further offset the small penalty in fill factor. Each cell is made up of 10μm pixels and subtends about 2.6 $'$ on the sky at the plate scale for Pan-STARRS,[2] which is $0.26''$ per pixel. The basic idea of the OTA is described at length in Tonry et al. 2002.[3,4]

Figure 1. The OTA is divided into 64 multi-function 600×600 CCD cells.

The division of the device into small cells also results in other advantages. We have designed the logic so that a cell which has a catastrophic short circuit can be isolated and will not affect the performance of the rest of the device's area. This is allowing us to improve the yield of these devices to better than 50% with a corresponding reduction in production cost. Each cell comprises 1.6% of the area, so that the loss of one or two is not a significant reduction in filling factor. In any wide field imager bright stars are a nuisance which pollute a large area around them. We will designate cells containing bright stars as "guide cells" and rapidly read out subarrays around the bright star for guiding (and thereby mitigate the charge pollution which would otherwise take place). Obviously we will read out cells in parallel which enables us to shorten the readout time. The division of the focal plane into 2.6 $'$ tiles also

Figure 2. CCID58 5K $\times$ 5K imager.

permits us to remove image motion on that scale using the "orthogonal transfer" (OT correction) feature - we have created a rubber focal plane which can differentially correct for atmospherically induced image motion.

A camera composed of OTAs automatically functions as a telescope guide camera without additional detectors or controllers. If multiple guide stars are selected, as in the figure above, then the guide signal is typically an average or median of the positions of all the stars. As the camera shutter opens, OTA detectors can already begin reading their designated guide cells at a high (e.g. 30 Hz) video frame rate. Another gain in etendue equivalent to shorter read time is achieved by opening the instrument shutter early and using OT correction to counter initial small amplitude telescope settling.
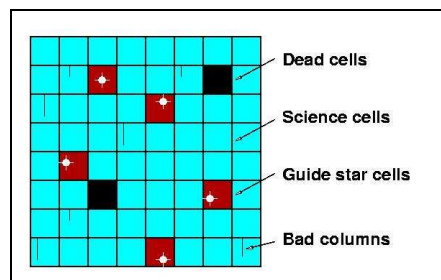
2. OTA ARCHITECTURE UPDATE

The development philosophy of improving overall system throughput rather than the usual path of high performance at a high cost results in our unusual design and architecture. Yield/cost and telescope etendue were treated as equally important figures of merit.

2.1 Low Cost and High Yield

The division of each device into 64 small CCDs or cells has resulted in a high, greater than 50% yield, as was predicted. For example, most recently, the third lot of CCID58 devices, now in the front illumination steps of processing at the Lincoln Lab, currently has a yield of 61%.

2.2 4-side Buttable Package

Certain aspects of the design were driven by the obvious need to close-pack the devices in a mosaic focalplane. We have created a custom package which uses a ceramic part which brings bond pads along one edge to a pin-grid array on the bottom. The ceramic also carries decoupling capacitors and JFET source followers for each video output. The silicon is glued to a molybdenum (gold plated) part which has three legs to provide a quasi-kinematic mount for bringing the focal plane to an accurate figure. The pin-grid array plugs into a flexprint for subsequent connections.

2.3 Deep Depletion and Charge Diffusion

The two design features which were most unusual were running metal connections in two criss-crossing layer over the pixels (in order to minimize the gaps between cells), and the "deeper depletion" implant which permits the logic to be isolated from the pixel's buried channel and the backside surface from both. Both of these have caused no loss in yield and appear to function very well. In particular, the deeper depletion implant allows us to run parallel gate voltages below ground, even though the logic is NMOS built right on the same silicon. It also allows us to fully deplete the CCD even if it is unusually thick (75um) in this case, and also achieve good charge diffusion. Since the QE in the far red is mostly a function of the increasing transparency of silicon, the thicker the device the higher the QE.

2.4 On-chip Guide

2.5 On-Chip Tip-Tilt Fast Image Correction

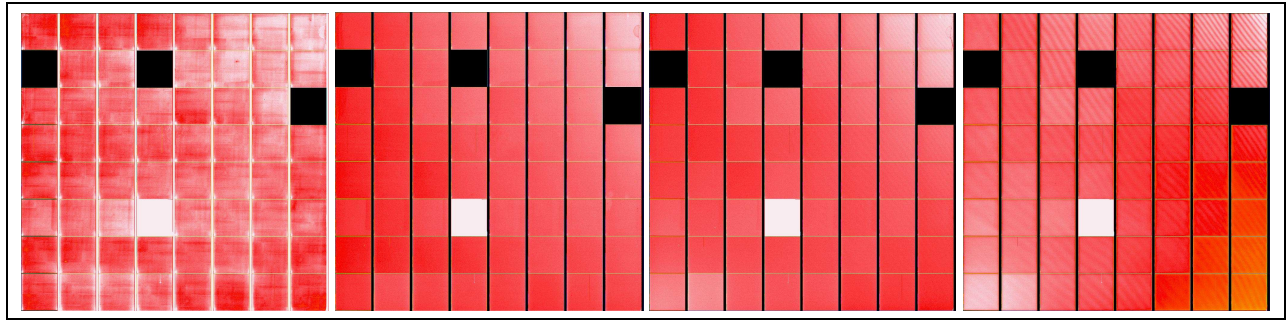## 2.6 Quantum Efficiency, Red Response

Figure 3. OTA flatfields at 400, 600, 800nm, and 1μm

The monochromatic flatfields in figure 3 show the usual MIT Lincoln Lab "brick wall" pattern at 400 nm from the step-and-repeat of the passivation laser, and they show fringing at 1 μm which reveal that the epoxy between CCD and handling wafer is too thick. The table shows representative QE values for OTAs which are thinned to 45 μm (and no substrate bias applied) and OTAs which are thinned to 75 μm (with a -20V substrate bias applied to fully deplete the CCDs and improve the charge diffusion).

The QE of the 45 μm thick OTAs is virtually identical to CCID20 devices whose QE has been determined by us and others have measured with completely different apparatus. However, the 75 μm thick OTA has a markedly improved red response beginning at about 750nm. By wavelengths of 1 μm, the 75 μm thick device has a 50% higher QE than the 45 μm thick OTA, as expected from the increased pathlength for IR photons.

Wavelength	45μm QE	75μm QE
400 nm	0.46	0.35
500 nm	0.62	0.62
600 nm	0.77	0.79
700 nm	0.89	0.93
800 nm	0.89	0.98
900 nm	0.70	0.88
1000 nm	0.24	0.37
1050 nm	0.075	0.11

Figure 4. Quantum Efficiency

ID resistors RTD for thermal

The OTA package includes an RTD for reading the temperature of the package itself. Current CCID58 designs require from 1.6 to 2 Watts to operate, but the power dissipation can be reduced during integration by lowering the output drain potential. We have made preliminary tests to use this as a method of regulating focal plane temperature in GPC1.

Package Pre-dishing

There is a CTE mismatch between the molybdenum package material and silicon which might cause mechanical doming of the silicon at the desired operating temperatures of approximately -65°C. To prevent this, the packages were pre-dished so that they would be flat when cooled to their operating temperature. Because GPC1's dewar window is a powered lens, direct measurement would be difficult. The coplanarity and flatness of each device can be inferred from a comparison of the PSF's of multiple stars in the field of GPC1.

Metal over Gates

Space was needed between for each cell's logic lines. Metal lines connect from the bond pads on one side of the device to all the cells. Using the space between the cells would have resulted in a significant loss of fill factor. Instead, two layers of criss-crossing lines were used. Vertical lines run right over the gates (or under the pixels, when back-illuminated.) There have been no apparent yield losses due to this decision, despite early concerns.[5]

Another effect of the metal is that the silicon becomes more and more transparent redward of 900 nm, and the reflection off of the metal becomes visible. The images above show the left-most 60 columns of a device where the first 19 columns are covered with metal. Their presence is obvious at 1um.

Figure 5. Effect of Metal Traces over Pixels.

A line cut through the images from the previous slide makes it easier to see the quantitative effect of the metal. It is immediately apparent that this is not a big effect. There is a curious reversal in the effect between 950 and 1000nm which we think must be some sort of interference effect in the epoxy which connects the CCD to its handling wafer. The most surprising thing is that the metal actually **decreases** the sensitivity of the pixels above. We regard this with some trepidation, because we think it may mean that the metal actually is shadowing a general glow coming from the reflection off of the silicon-epoxy interfaces, and this glow is probably a bad thing because it creates a psf with a very large halo. We have not yet done experiments with monochromatic psf's at red wavelengths, but we should. We have also taken steps to reduce the thickness of the epoxy between the CCD and handling wafer.
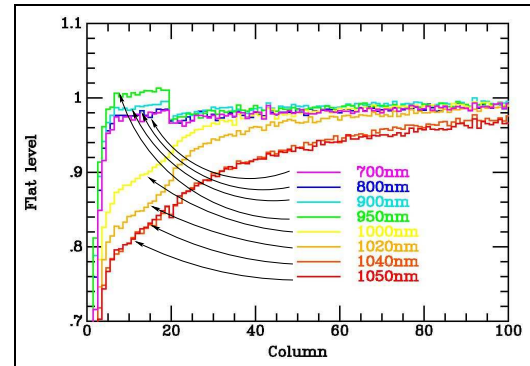
3. A DETECTOR FOR PAN-STARRS

The biggest technological challenge for Pan-STARRS is the detectors. We require in excess of 1 billion pixels in each of four focal planes, and we also require exposures of 30 seconds or less, which puts an extreme burden on the readout electronics if we are to achieve a reasonable duty cycle. For example, at the 10 cents per pixel cost of IR detectors, it would cost a half billion dollars to equip all four focal planes. We therefore are striving to produce these cameras which comprise 10x as many pixels as have ever been deployed before using CCD devices at 1/10 the cost per pixel and at 10x the readout speed. The key to this we believe is the concept of a monolithic array of CCDs. In this case an 8x8 array of CCDs, each of which is approximately 600x600 pixels. In order to address these CCDs, each is equipped with logic which isolates it or connects it to the output circuitry.

4. CURRENT PERFORMANCE ON PAN-STARRS 1

4.1 CCID58 Linearity and Full Well

Because of the OTA's high channel count, and its typical use in a large mosaic such as the Giga Pixel Camera, traditional means of analyzing and optimizing detector performance are often impractical. Two sets of software were employed for tasks of selecting and characterizing these CCDs. The OTA Test Bench (OTB) has been described in detail. More recently, tests for properties like linearity have been carried out in situ, with the devices installed in GPC1 itself. This is made possible by various built-in calibration sources, such as LEDs which are under control of the STARGRASP CCD controller, and by similar scripts to those used with OTB which loop through the thousands of CCD cells and plot their response in a comprehensible way.

Although not discernible at the reduced size of the figure, the vertical scales on the 60 graphs represent % linearity from -2% to +1%, and the x-axis ranges from 0 to 65,000 ADU. We chose to set our system gain to 1e-/ADU for CCID58 devices because the usable full well had already been determined to be below 65,000. (This was lower than designed and improvements are
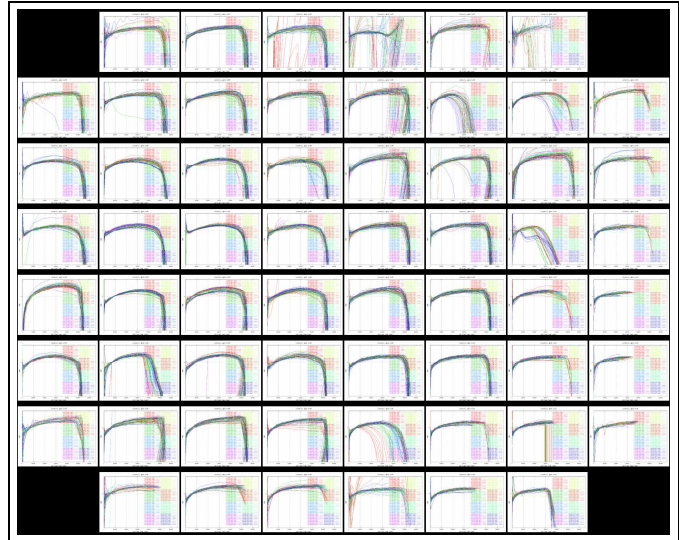

Figure 6. Linearity graphs generated by GPC1 characterization tools. The task of characterizing Giga Pixel 1 necessitated coming up with new ways to visualize detector performance.

expected for the CCID64 OTA.) Each graph contains 64 lines – one for each cell in the OTA. As can be seen from the graphs, the cells have linear response up to at least 45,000 e-, though there are some outliers. Outliers could be bad cells, or cells not sufficiently illuminated by the calibration LEDs. We intend to improve this in future versions, by allowing the tools to filter out the known bad cells from the graphs.

4.2 CCID58 Lot 2 Readout Performance

A set of 60 OTA devices, when read simultaneously in GPC1 at Pan-STARRS 1, achieve noise performance of 7 e- RMS across an entire bias readout of each cell. A phase shift in the clocking and sampling times between sets of devices was implemented to reduce or eliminate self generated crosstalk in signal paths external to the OTA occurring as a result of reading 480 outputs simultaneously.

In the timespan 7.7 seconds (less than a second per each of the 8 sequentially read cell rows) all 3840 cells of GPC1 are read and completely saved on disk. 85% of these cells have a read noise of less than 7 e-. At the Lincoln Lab, read singly with a favorable system gain, OTAs were shown to meet the goal of a 5e- or less readnoise. (ref.)

The current OTA speed and noise performance is the result of an ongoing optimization process. In addition to clocking pattern, voltage, and phase tuning, this process has included steps to mitigate radio interference on the order of $1 Watt/m^2$ from the near field of transmission towers. Computer and network interfaces were also tuned to keep up with the data stream, resulting in 7.7 seconds for the current *system* performance time for repeated readouts.
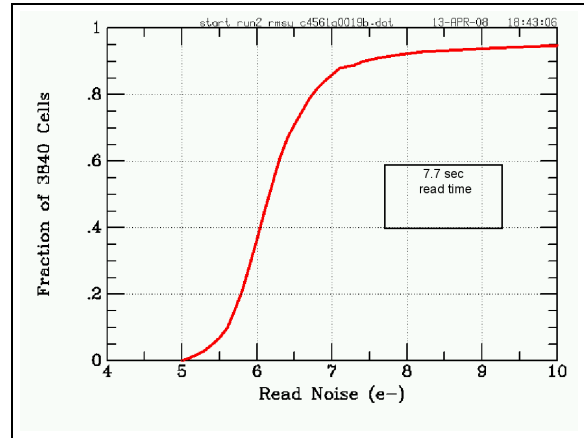
Figure 7. Cumulative Histogram of Read Noise

4.3 CCID58 Dark Current
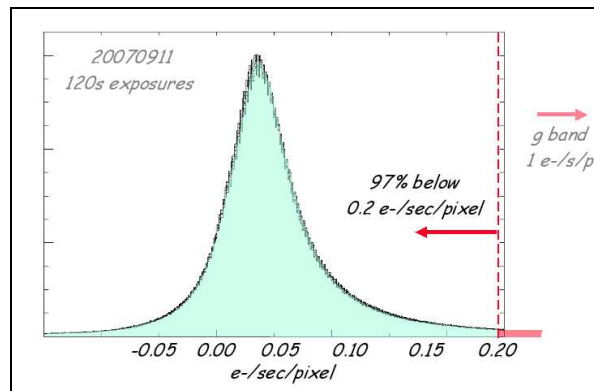
Figure 8. Dark Current.

The dark current of the CCID58 was expected to be very low, and has been measured and found to be below 0.2 e-/sec on the devices selected for and installed on the Giga Pixel Camera 1.

4.4 Anomalies

Shortcomings of the current development lots have been identified on the "OTA Test Bench" in Manoa and also in the Giga Pixel Camera 1 installed on Pan-STARRS 1 on Maui. This section discusses the nature of known OTA anomalies, and specifically those of the current CCID58 generation which are installed in GPC1.

Molybdenum Package vs. Silicon

Molybdenum used for the CCID58 package has a coefficient of thermal expansion of about $4 \times 10^{-6}/°$C, while silicon is about $2.5 \times 10^{-6}/°$C. This might cause doming of the silicon at operating temperatures. To counteract this, a pre-dishing step is included in manufacturing. See also the discussion of a new package for CCID64 which addresses this issue. We have relatively precise metrology of the OTAs and the GPC1 focal plane at room temperatures, but measurement at

GPC1 operating temperature has only been determined indirectly, through PSFs of focus sequences. This analysis is still on-going, but the OTAs appear to be sufficiently flat at $-70C$.

Corner CTE Problem

A defect resulting from ionization in a processing step during manufacture at Lincoln Lab affects all CCID58 devices of the first two lots, to varying degrees. This includes all of the devices currently installed in GPC1. The defect typically renders between 3 to 10 cells in one corner (the corner which was closest to the edge of the wafer from which the OTA was made) to be unusable due to very poor parallel CTE, or residual charge. This effect is seen in areas of the cell **not** under the metal traces. See also, the discussion of the third CCID58 lot and CCID64. The former should produce up to 20 new devices which we plan to install in GPC1 to address this issue.

Negative Substrate Defects

Very low negative substrate voltages (up to -40 Volts) should result in excellent, low charge diffusion. However, there is a tradeoff between this improvement in charge diffusion and the rate at which defects leak charge, which results in bright image artifacts.
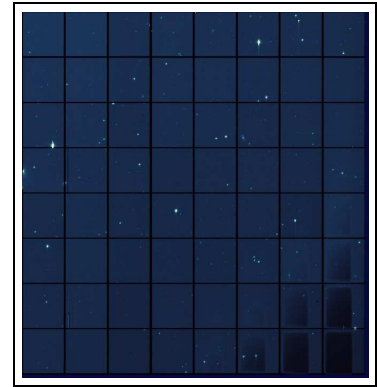

Figure 9. "Corner CTE" Defect

5. FUTURE DEVELOPMENT

The next step in OTA development is the CCID64. The first design and production run intended to improve noise performance, increase full well, and fix the corner CTE problem. The read noise change is a two stage output amplifier with a first stage source follower with pJFET driver plus active load and a second stage source follower buried-channel MOSFET.

5.1 Improved Performance

CCID58 lot 3 Fixes Problems

omit (just talk about CCID64)

CCID64 Greater Full Well

Increased full well from thinner gate dielectric and greater implant

Bad Corner CTE Fix

Two methods were employed to fix the CCID58 corner CTE problem Since the problem was not present in the metal over gates areas of the OTA, metal was put across the whole device. The second fix addressed a problem with space charge during etching. Unfortunately, a mechanical malfunction scratched all the wafers and it appears that no OTA will be fully functional. We should, however, be able to evaluate the success of all of the design changes on the cells that are operable.

Simplification

Past OTA lots have included many splits. We now understand the effect of most of the choices so that the latest lots can begin to be more uniform. Early OTAs had both 12 and 10μm pixel sizes.

At some point, too small a pixel size would start to become a problem because ..... There was no difference in yield in the 10μm devices when compared to the 12μm devices which were manufactured. All CCID64's will have 10μm pixels, like their CCID58 predecessors. All CCID64's will have only 2-phase serial registers with a serial dump gate feature. CCID58's were a mix of 2-phase and 3-phase. All CCID64's are planned with "Type I" 4-phase OT pixels. Some previous OTAs had the "Type II" pixel structure with 4 triangles.

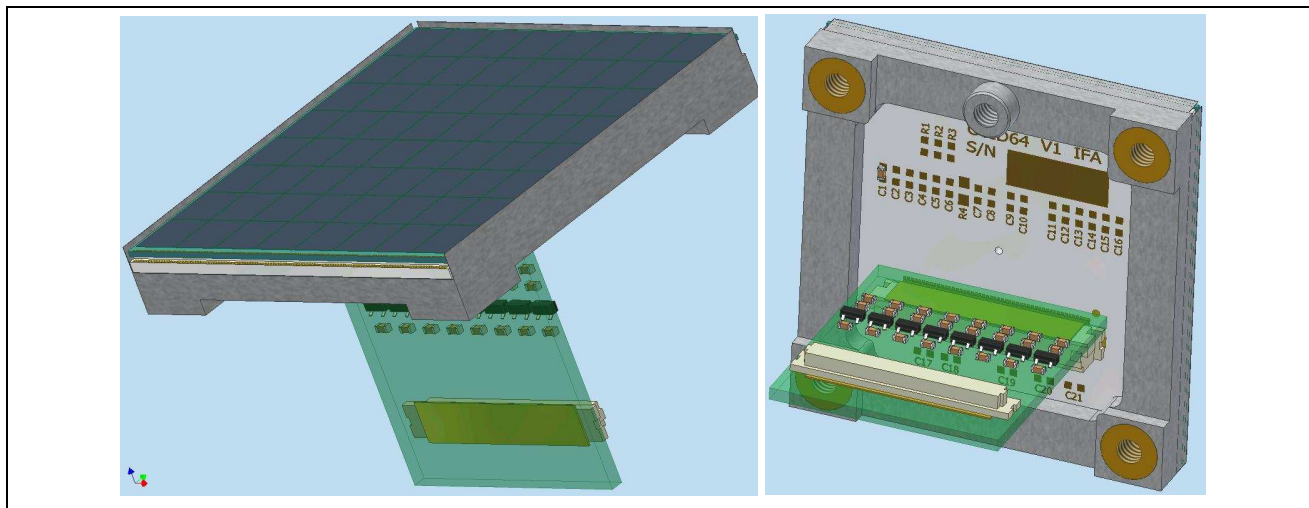## 5.2 New package and features

Figure 10. Two views of CCID64 package design showing handling bumpers and surface mount connector on the bottom.

CCID64's package design and composition will differ from the CCID58. As required, packages are still 4-side buttable, but the design includes handling bumpers shown in 10. Also, aluminum nitride ceramic was chosen instead of molybdenum. AlN has a much better CTE match. In units of $10^{-6}/^{\circ}$C, both AlN and Silicon have a CTE of about 2.5 compared to 4.0 for Moly. This will also remove the need for pre-dishing the package surface. The AlN piece will also have a surface mount connector soldered directly making it a single piece rather than a two piece assembly.

6. CONCLUSIONS

The OTA detector was designed to meet the needs and budget of the Pan-STARRS project. The second lot of the CCID58 model is now being used successfully to obtain on-sky data. A third lot of the CCID58 is in production and, at the stage of front illumination processing, has a yield of better than 60% and appears to have addressed the corner CTE problem successfully. A future CCID64 with improvements in quality and performance, its package, and new features is in development.

ACKNOWLEDGMENTS

REFERENCES

[1] J.L. Tonry, et al. The Orthogonal Transfer CCD *PASP* 109:1154, 1997.

[2] N. Kaiser. Pan-STARRS: a wide-field optical survey telescope array. *Proceedings of the SPIE*, 5489:11–22, 2004.

[3] J.L. Tonry, et al. Giga-pixels and Sky Surveys *Scientific Detectors for Astronomy 2002, Astrophysics and Space Astronomy Library*, 300:395, 2004.

[4] J.L. Tonry, et al. Rubber Focal Plane for Sky Surveys *Proceedings of the SPIE*, 4836:206, 2002.

[5] B.E. Burke, et al. The orthogonal-transfer array: a new CCD architecture for astronomy *Proceedings of the SPIE*, 5499:185, 2004.

[6] P.M. Onaka, et al. IOTA: the array controller for a gigapixel OTCCD camera for Pan-STARRS *Proceedings of the SPIE*, 5499:4990, 2004.

[7] J.L. Tonry, et al. The Orthogonal Parallel Transfer Imaging Camera *Scientific Detectors for Astronomy 2002, Astrophysics and Space Astronomy Library*, 300:385, 2004.